Coactivation of Thalamic and Cortical Pathways Induces Input Timing-Dependent Plasticity in Amygdala

Jun-Hyeong Cho, Ildar T Bayazitov, Edward G Meloni, Karyn M Myers, William A Carlezon Jr., Stanislav S Zakharenko and Vadim Y Bolshakov

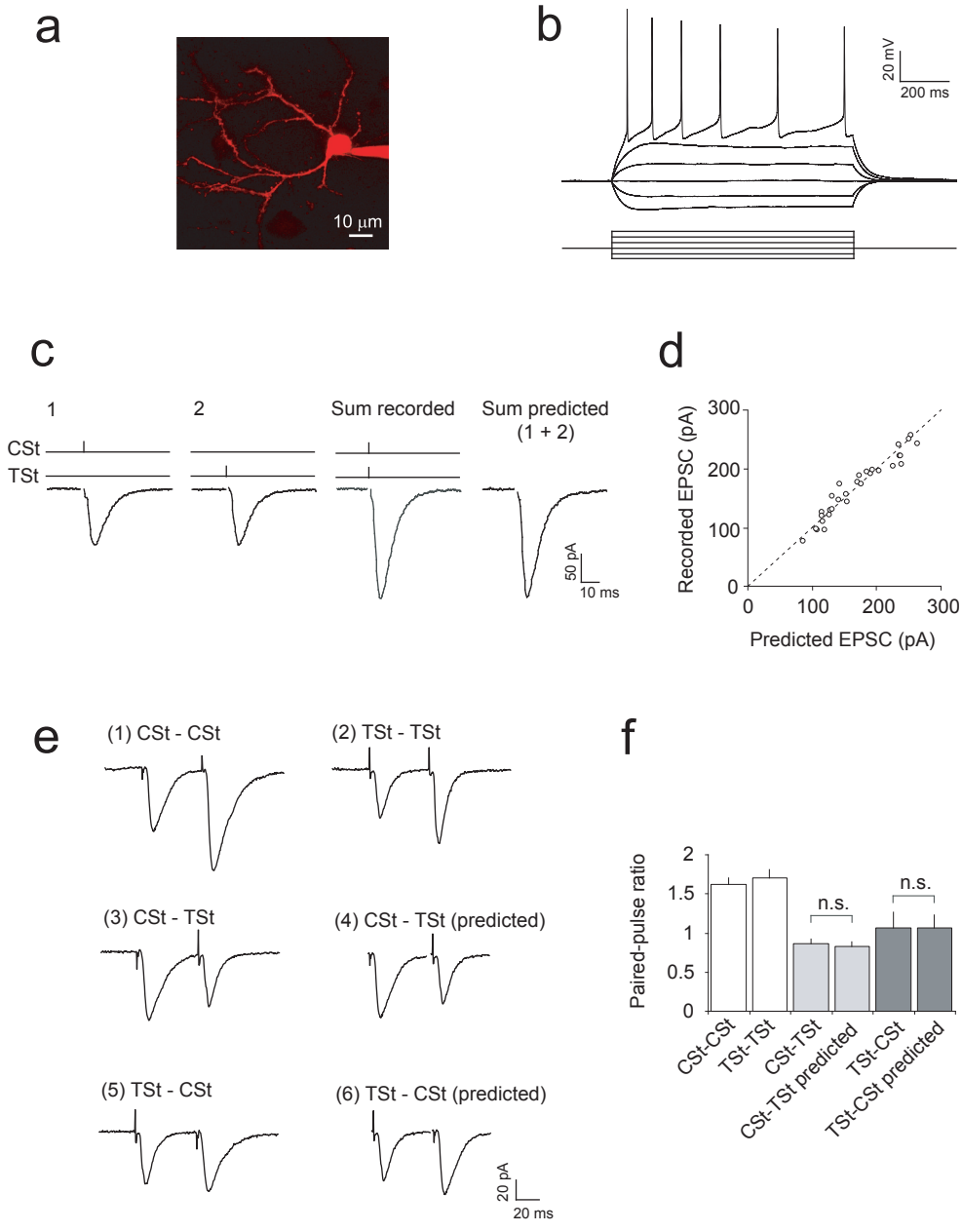

Supplementary Figure 1. Independent activation of cortical and thalamic inputs to the same neuron in the LAn. (**a**) Two-photon microscopic image of the LAn neuron loaded with Alexa594. (**b**) Responses of a cell in the LAn to prolonged current injections in current-clamp mode. Spike frequency adaptation indicates that the recorded cell was

principal neuron. (**c**) EPSCs evoked by stimulation of cortical (1) or thalamic (2) inputs individually, and when both inputs were activated simultaneously (sum recorded). The last trace (sum predicted) is the arithmetic sum of the individual evoked responses. Five EPSCs were recorded and averaged for each stimulation condition. (**d**) The amplitudes of recorded combined EPSCs (y-axis) were plotted versus predicted EPSC amplitudes (x-axis) in a scatter plot. Linearity of the relation between the amplitude of the recorded combined EPSC and the predicted EPSC amplitude (correlation coefficient, $r = 0.97$) indicates that the inputs were activated independently. (**e**) Cortical and thalamic inputs to the LAn do not demonstrate cross-facilitation. Both cortico-LAn (1) and thalamo-LAn EPSCs (2) showed significant PPF (50-ms interstimulus interval; no significant difference in the magnitude of PPF between two pathways, n = 9, paired *t* test, $P = 0.55$). Stimulation of the cortical input with a single stimulus had no effect on the amplitude of the EPSC in the thalamic input evoked with a 50-ms delay (3), and vice versa (5). The predicted paired-pulse ratio (PPR, a ratio of the first EPSC in one pathway to the first EPSC in another pathway recorded during paired-stimulation) was estimated under the assumption that stimulation of either pathway is independent (traces 4 and 6). The predicted PPR was then compared to the recorded PPR, when two inputs were stimulated by single pulses sequentially with a 50-ms delay. Ten synaptic responses were averaged for each stimulation condition. In these experiments, the external Ca^{2+} concentration was 1 mM. (**f**) Summary of the experiments as in (**e**). The recorded and predicted PPR magnitudes were not different (CSt-TSt: n = 8, *t* test, $P = 0.40$; TSt-CSt: n = 4, *t* test, $P = 0.94$). Error bars indicate s.e.m.

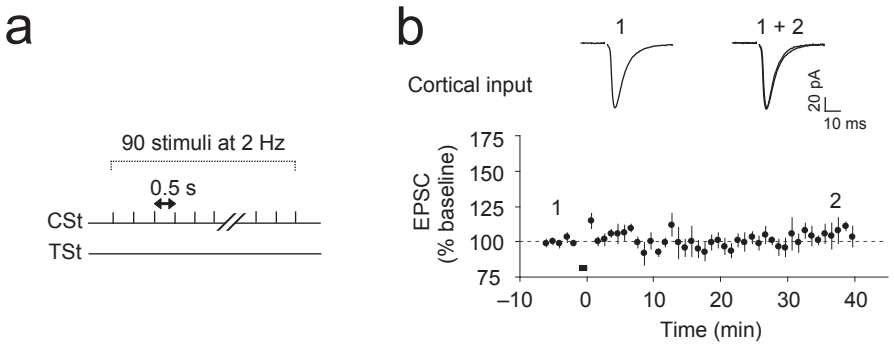

Supplementary Figure 2. Stimulation of the cortical input alone at 2 Hz does not induce synaptic potentiation. (**a**) Design of experiments in which stimulation of thalamic input was omitted and cortical input was stimulated at a 2-Hz frequency. (**b**) Cortico-LAn EPSCs were not potentiated if cortical input was stimulated alone for 45 seconds at 2 Hz (n = 5, paired *t* test, $P = 0.62$ versus baseline). Error bars indicate s.e.m.

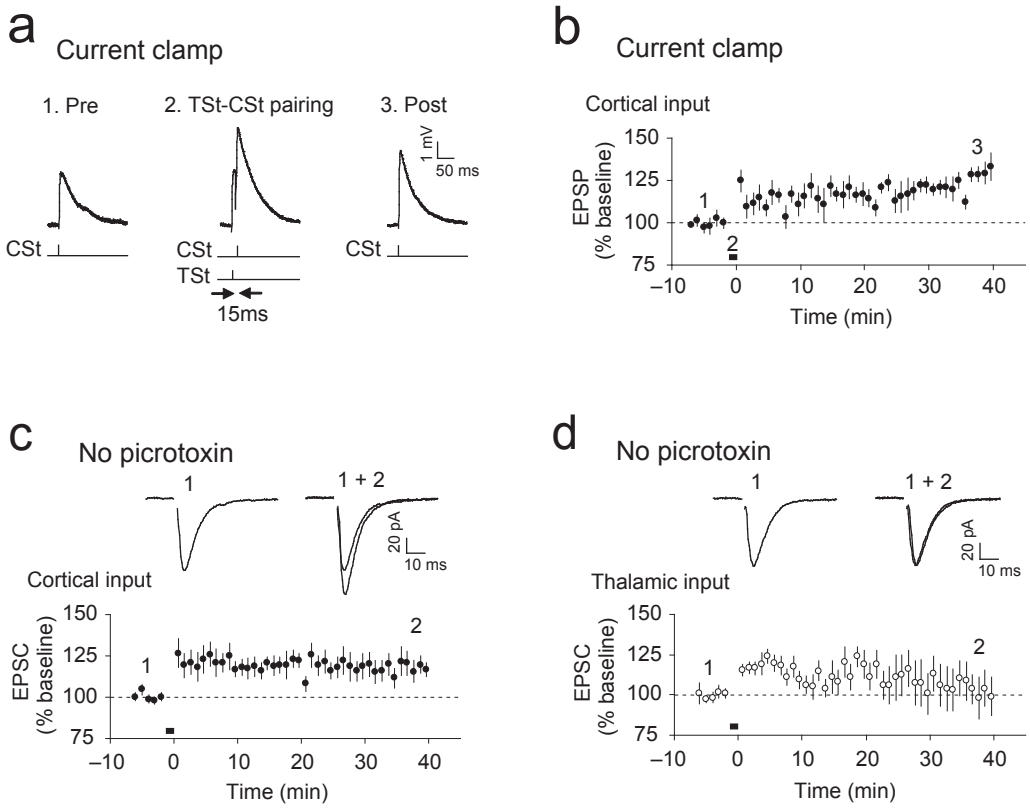

Supplementary Figure 3. Properties of ITDP in inputs to the LAn. (**a** and **b**) TSt-CSt pairing protocol induces ITDP of cortico-LAn EPSPs. (**a**) EPSPs evoked by stimulation of cortical input during baseline recording (1) and after the delivery of TSt-CSt pairing protocol (3). Trace in the middle (2) shows responses evoked by paired stimulation of thalamic and cortical inputs with a 15 ms interpulse interval. (**b**) ITDP of the cortico-LAn EPSP is induced under current-clamp recording conditions (n = 6, paired *t* test, $P < 0.001$ versus baseline). (**c**) ITDP in cortical input is induced normally with $GABA_A$ receptor-mediated inhibition intact (without picrotoxin in the external solution) (n = 8; paired *t* test, $P < 0.05$ versus baseline amplitude). Insets show the average of 10 cortico-LAn EPSCs recorded before (1) and after (2) the induction of ITDP in voltage-clamp mode. (**d**) No potentiation was still observed in the priming thalamic input (same experiments as in (**c**), n = 8, $P = 0.68$ versus baseline). Error bars indicate s.e.m.

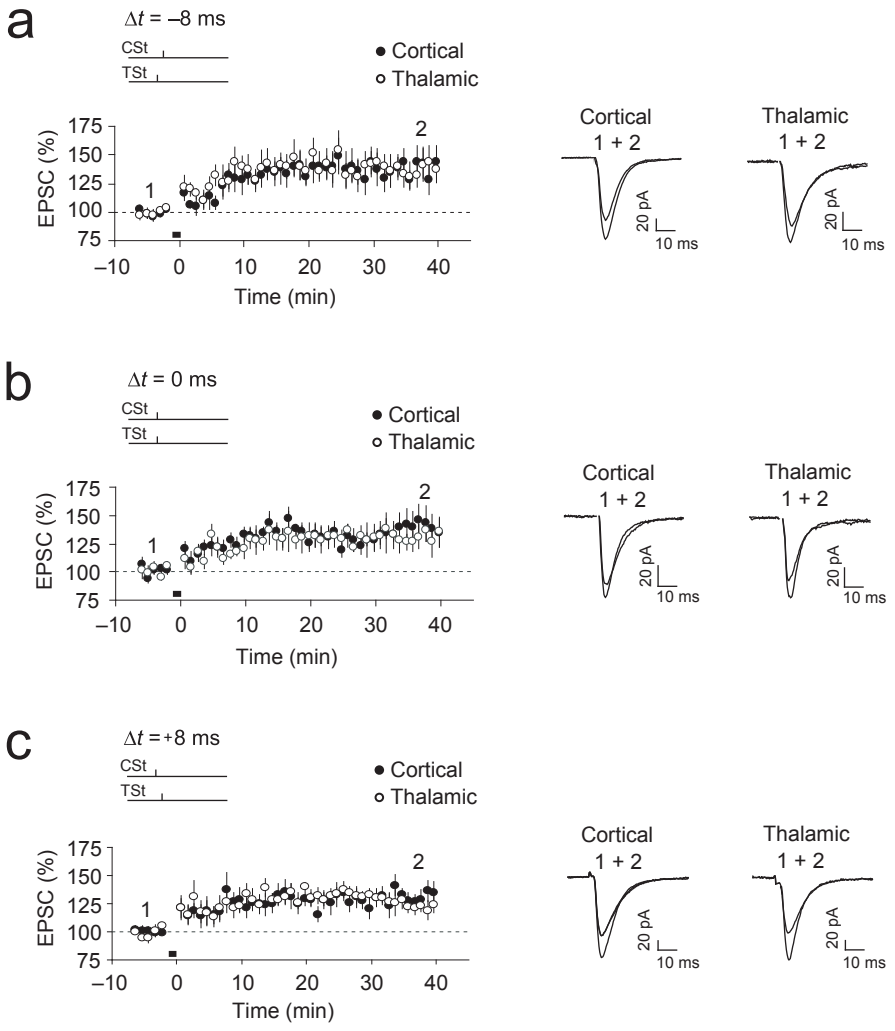

Supplementary Figure 4. Induction of ITDP at short time intervals between thalamic and cortical stimuli. (**a**) Summary graphs of ITDP experiments with time interval of –8 ms during the TSt-CSt paring showing the time course of the EPSC amplitude changes following repetitive paired activation of thalamic and cortical fibers (n = 6, $P < 0.05$ versus baseline for both cortical and thalamic inputs). Traces are averages of 15 EPSCs recorded in individual experiments before (1) and after (2) the repetitive coactivation (black bar) of thalamic and cortical inputs. (**b**) Same as in (**a**) but with time interval of 0 ms during the TSt-CSt paring (n = 6, $P < 0.05$ versus baseline and $P < 0.01$ versus baseline for potentiation in cortical and thalamic inputs, respectively). (**c**) Summary graphs of ITDP experiments with time interval of +8 ms during the CSt-TSt paired stimulation where the order of stimulation pulses was reversed compared to (**a**) (n = 6; cortical input, paired *t* test, $P < 0.05$ versus baseline; thalamic input, $P < 0.01$ versus baseline). Error bars indicate s.e.m.

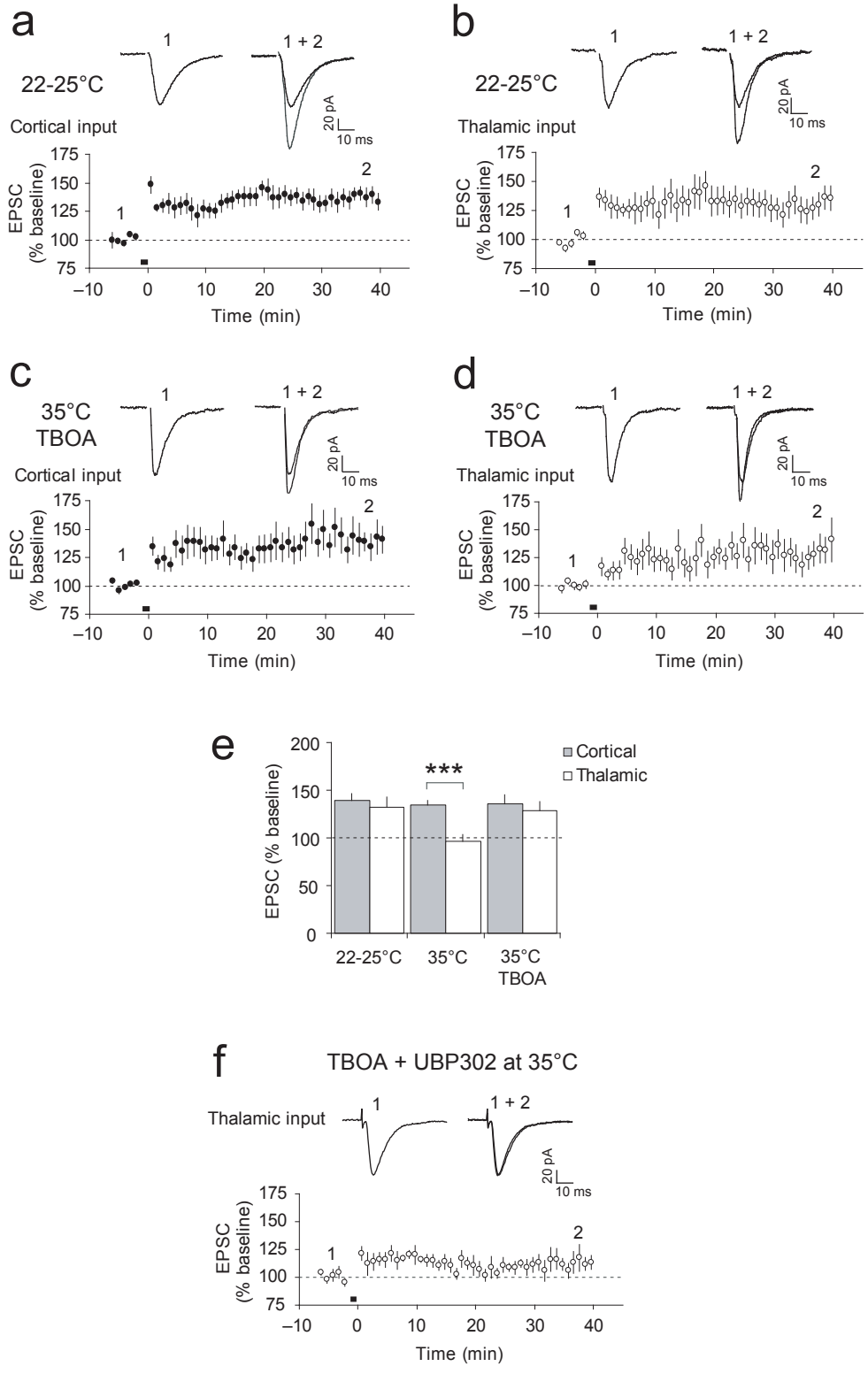

Supplementary Figure 5. Active glutamate uptake maintains pathway specificity of ITDP in the LAn. (**a**) TSt-CSt pairing-induced ITDP (Δt = –15 ms) in cortical input to the LAn at room temperature (22-25°C, n = 14, $P < 0.001$ versus baseline, paired *t* test). Insets show the average of 15 cortico-LAn EPSCs recorded before (1) and 35-40 min after (2) the TSt-CSt paired stimulation at a holding potential of –70 mV. (**b**) Synaptic responses in thalamic input

recorded in the same experiments as in (**a**) (n = 14, $P < 0.05$ versus baseline). Pathway specificity of ITDP was lost when the TSt-CSt pairing protocol was delivered at room temperature. (**c** and **d**) Inhibition of glutamate uptake with DL-TBOA (10 μM) at 35°C resulted in the loss of pathway specificity of ITDP. The TSt-CSt pairing protocol induced LTP at both cortico-amygdala synapses (**c**) (n = 9, $P < 0.01$ versus baseline) and thalamo-amygdala synapses (**d**) (n = 9, $P < 0.05$ versus baseline). (**e**) Summary of the EPSC amplitude changes in cortical and thalamic inputs following the TSt-CSt paired stimulation under different experimental conditions. Results of the ITDP experiments shown in Figures 1e and 1f, demonstrating that ITDP was pathway-specific at physiological temperatures (without DL-TBOA in the bath solution), were also included in this graph (middle). ***$P < 0.001$ for the EPSC amplitude (% baseline) in cortical versus thalamic input. (**f**) UBP 302 (10 μM) blocked heterosynaptic potentiation in thalamic pathway following the delivery of the TSt-CSt paired stimulation in the presence of DL-TBOA (10 μM) at 35°C (n = 6; paired *t* test, $P = 0.14$ versus baseline). Error bars indicate s.e.m.

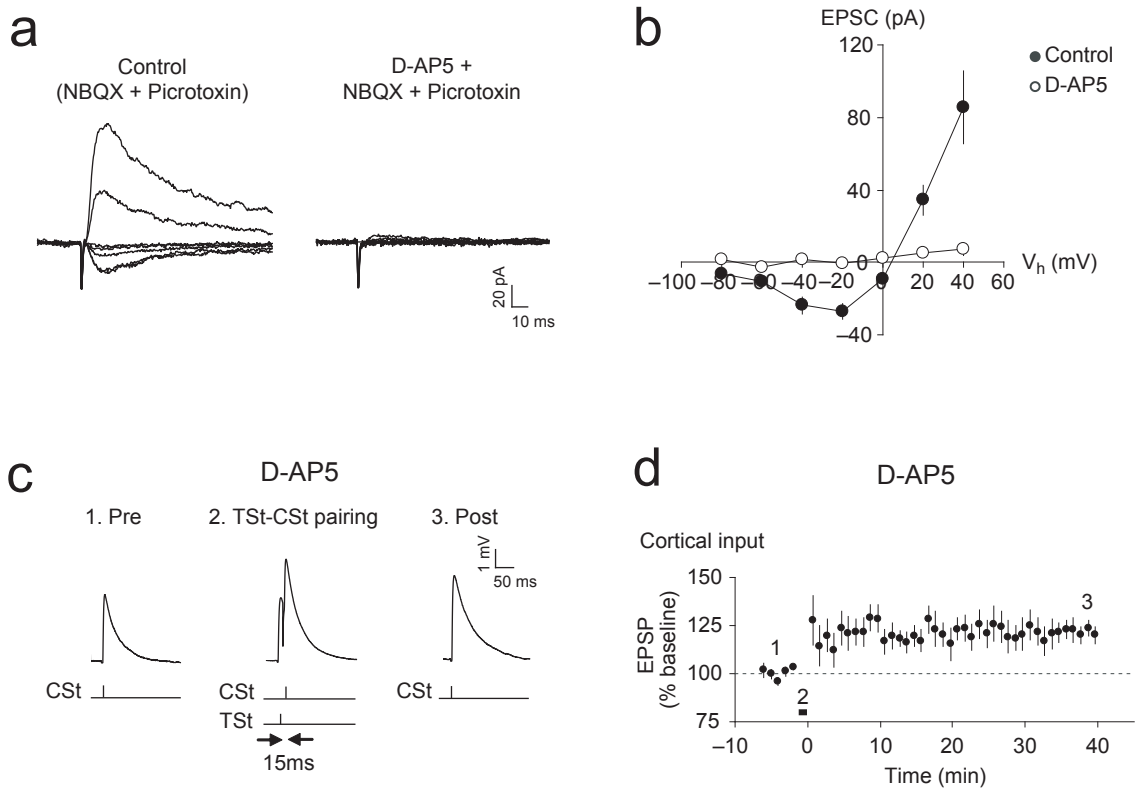

Supplementary Figure 6. ITDP of the cortico-LAn EPSP is not prevented by NMDA receptor blockade. (**a**) NMDAR EPSCs in the cortical input to the LAn (left) were blocked by 50 μM D-AP5 (right). In these experiments, the EPSCs were recorded in the presence of NBQX (10 μM) and picrotoxin (50 μM) at holding potentials ranging from –80 mV to +40 mV. Traces are averages of ten EPSCs recorded at each holding potential. (**b**) Current-voltage plot of the NMDAR EPSCs (as in **a**) recorded under control conditions (closed symbols) and in the presence of D-AP5 (open symbols). The EPSC amplitude was measured at the peak of the response. Control NMDAR EPSCs showed substantial voltage dependence, as they were blocked by external Mg^{2+} at negative holding potentials (n = 5). (**c**) EPSPs evoked by stimulation of cortical input and recorded in current-clamp mode in the presence of 50 μM D-AP5 during baseline recording (1) and after the delivery of TSt-CSt pairing protocol (3). Trace in the middle (2) shows responses evoked by paired stimulation of thalamic and cortical inputs with the 15 ms interpulse interval. (**d**) Addition of D-AP5 (50 μM) to the external solution did not prevent the induction of ITDP in cortical input under current-clamp recording conditions (n = 8, paired *t* test, $P < 0.01$ versus baseline). Error bars indicate s.e.m.

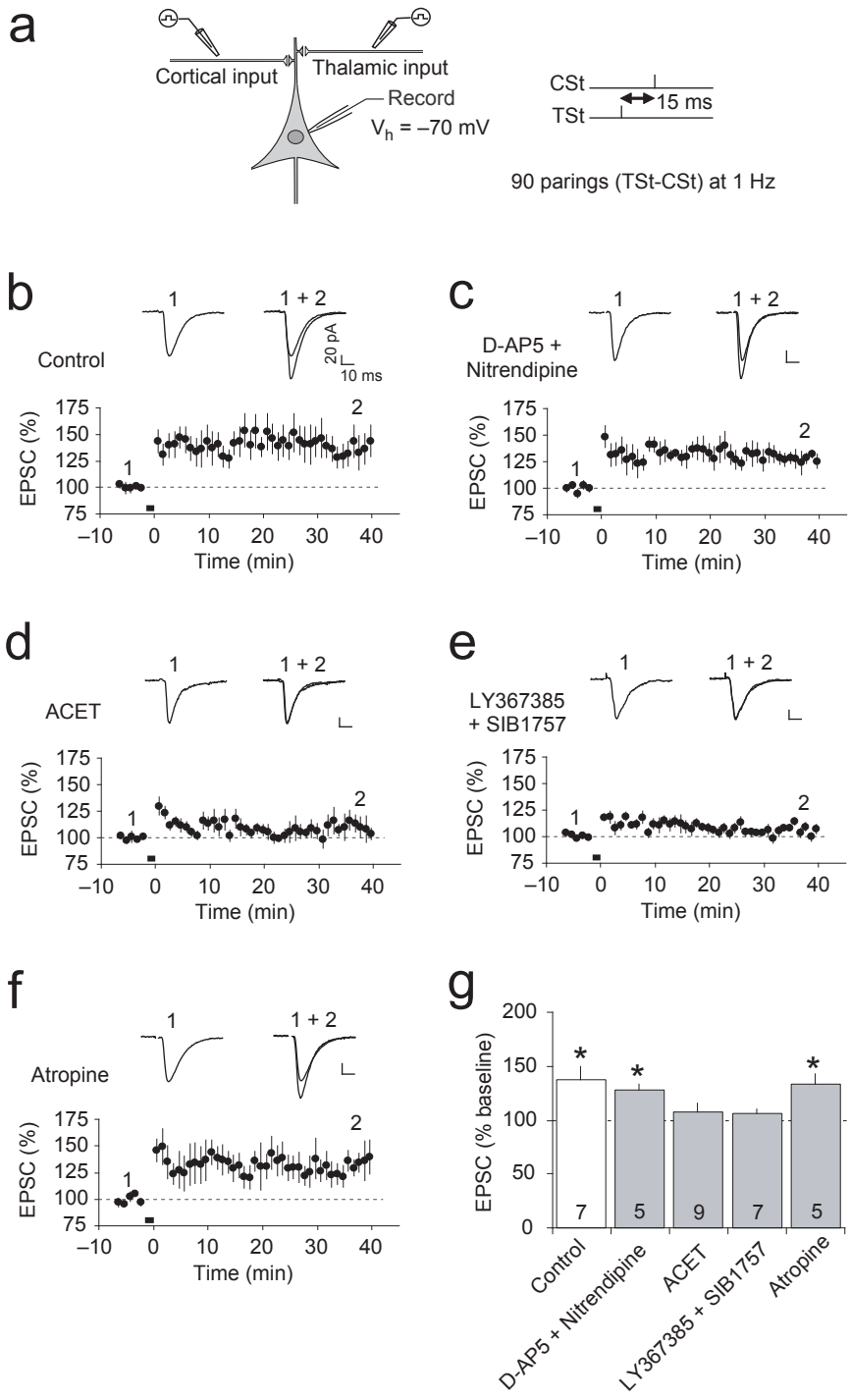

Supplementary Figure 7. Pharmacological characterization of ITDP at the cortico-LAn synapses. (**a**) Schematic representation of the experimental design (left) and a diagram illustrating the standard TSt-CSt pairing protocol that consisted of paired stimulation of thalamic and cortical inputs for 90 seconds at 1 Hz (right). Thalamic stimulus (TSt) was delivered 15 ms earlier than cortical stimulus (CSt). (**b**) The TSt-CSt paired stimulation induced ITDP in the cortical input to the LAn (n = 7, paired *t* test, $P < 0.05$ versus baseline). Insets show the average of 15 cortico-

LAn EPSCs recorded before (1) and 35-40 min after (2) the TCt-CSt paired stimulation (black horizontal bar). Scale bars here and for other traces in the figure: 20 pA and 10 ms. (**c**) In the presence of D-AP5 (50 μM) and nitrendipine (20 μM), the TSt-CSt paired stimulation also led to significant potentiation of the cortico-LAn EPSC (n = 5, paired *t* test, $P < 0.05$). The magnitude of ITDP under these conditions was not different from control ITDP (unpaired *t* test, $P = 0.48$). (**d**) ITDP at the cortico-LAn synapses was blocked in the presence of ACET (10 μM) in external solution (n = 9; paired *t* test, $P = 0.31$ versus baseline). (**e**) Joint application of group I mGluRs antagonists LY 367385 (100 μM) and SIB 1757 (30 μM) (inhibiting mGluR1 and mGluR5, respectively) blocked ITDP in cortical input (n = 7, paired *t* test, $P = 0.11$ versus baseline). (**f**) ITDP was unaffected by addition of the muscarinic acetylcholine receptors antagonist atropine (1 μM) to the external solution (n = 5; paired *t* test, $P < 0.05$; not different from the magnitude of ITDP under control conditions, unpaired *t* test, $P = 0.76$). (**g**) Summary of ITDP experiments. Numbers within each bar indicate the number of experiments for each condition. *$P < 0.05$, mean baseline EPSC amplitude versus EPSCs recorded 35-40 minutes after the TSt-CSt pairing, paired *t* test. Error bars indicate s.e.m.

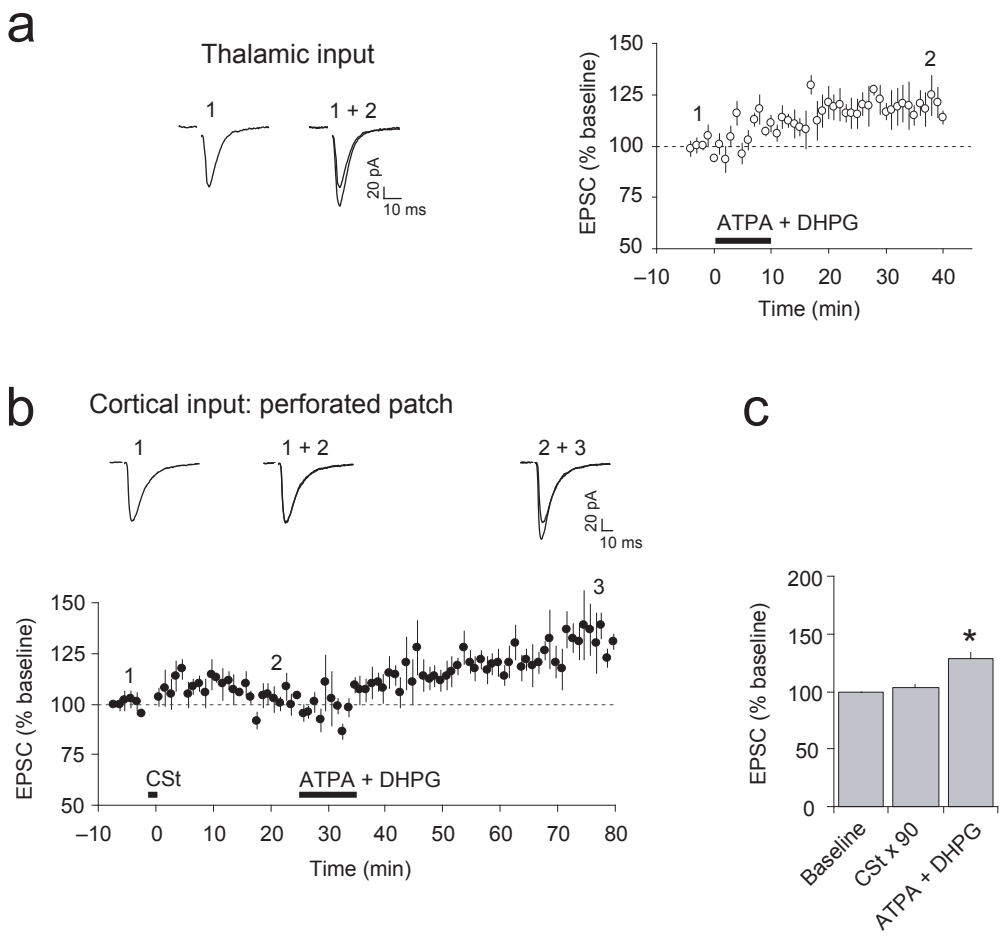

Supplementary Figure 8. Properties of potentiation in inputs to the LAn induced by ATPA+DHPG application. (**a**) Joint application of ATPA (1 μM) and (S)-DHPG (10 μM) for 10 min led to potentiation of the EPSC amplitude in thalamic pathway (n = 5; paired *t* test, $P < 0.05$ versus baseline; not different from potentiation in the cortico-LAn pathway, unpaired *t* test, $P = 0.88$). Traces (left) show averaged thalamo-LAn EPSCs recorded before (1) and 25-30 min after (2) ATPA and (S)-DHPG application. (**b**) The nystatin-based perforated patch-clamp technique was used in these experiments. First, the cortico-amygdala pathway was stimulated alone for 90 s at 1 Hz (CSt). Such stimulation did not result in potentiation of the cortico-LAn EPSC (n = 6, paired *t* test, $P = 0.34$ versus baseline at 20 min post-stimulation). Slice was then perfused with the external solution containing 1 μM ATPA and 10 μM (S)-DHPG for 10 minutes. The ATPA+DHPG application led to significant potentiation of the EPSC amplitude (n = 6; paired *t* test, $^*P < 0.05$ versus baseline at 40 min after ATPA and (S)-DHPG application). (**c**) Summary of the experiments as in (**b**). Error bars indicate s.e.m.

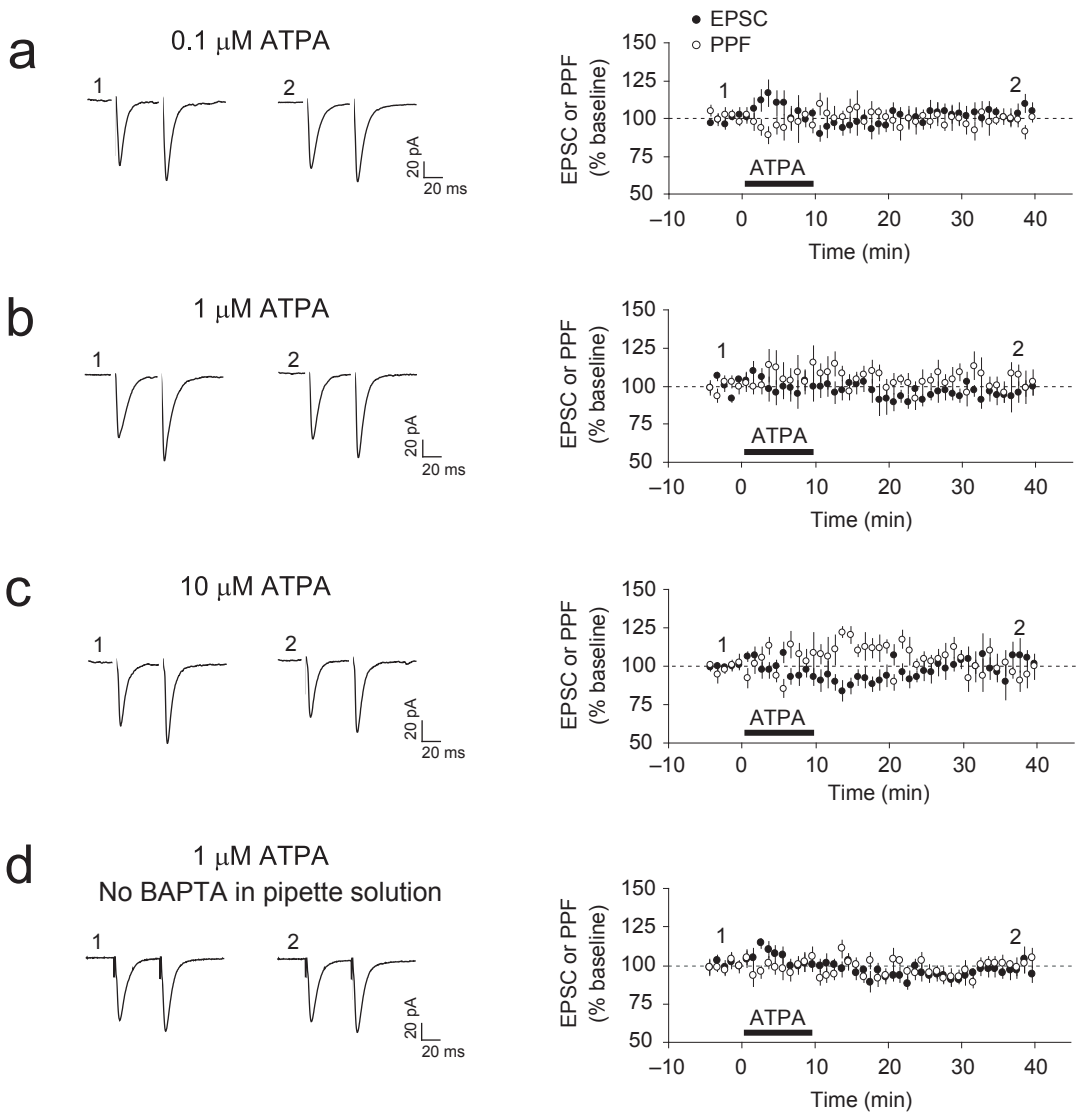

Supplementary Figure 9. Activation of GluR5 subunit-containing KA receptors with ATPA had no effect on the magnitude of PPF at cortico-LAn synapses. (**a**) Paired-pulse facilitation (PPF) recorded with a 50 ms interstimulus interval in cortical input to the LAn under baseline conditions and after ATPA (0.1 μM) application. Left, traces show averages of 15 EPSCs recorded before (1) and after (2) ATPA was applied. Right, summary graphs showing the time course of changes in the ESPC amplitude and PPF value following ATPA application (n = 6). (**b** and **c**) Experiments were performed as in (**a**) but with 1 μM ATPA (**b**, n = 7) and 10 μM ATPA (**c**, n = 8) in the external solution. BAPTA (10 mM) was included in pipette solution in the experiments shown in (**a**-**c**). (**d**) Experiments were performed as in (**a**-**c**) but without BAPTA in pipette solution. ATPA (1 μM) still had no effect on the PPF magnitude (n = 10, P = 0.62 versus pre-ATPA baseline). Error bars indicate s.e.m.

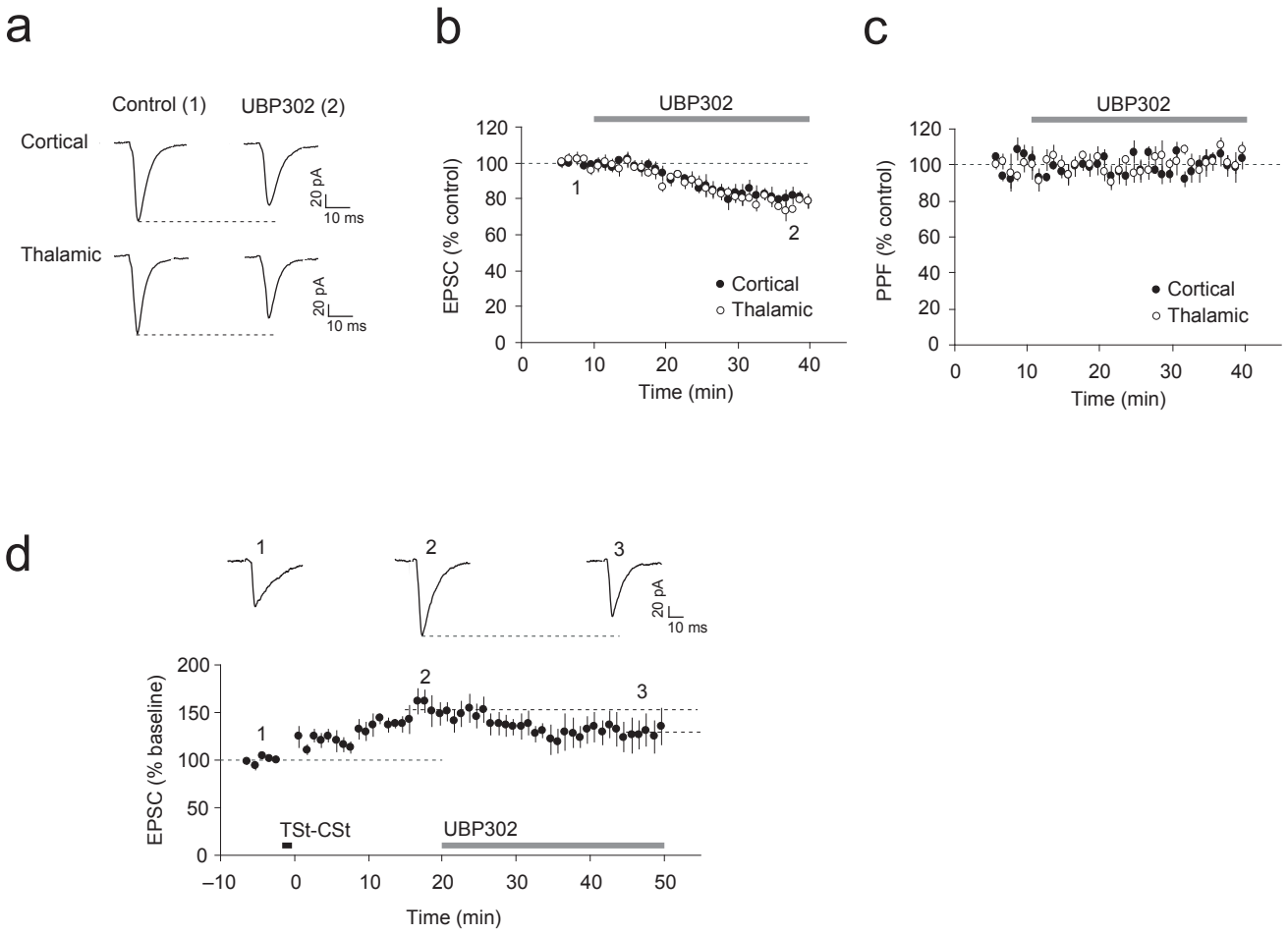

Supplementary Figure 10. Effects of UBP302 on EPSCs in inputs to the LAn. (**a**) Examples of EPSCs, recorded in LAn neuron, evoked by stimulation of cortical or thalamic inputs under control conditions (1) and after the application of 10 μM UBP302 for 25-30 min. Traces are averages of 10 EPSCs. (**b**) Bath-applied UBP302 diminished the EPSC amplitude in cortical (n = 6) or thalamic (n = 6) inputs to the LAn. (**c**) PPF, measured with a 50-ms interval), was unaffected by UBP302 at cortico-LAn or thalamo-LAn synapses (n = 6 for either pathway; paired *t* test, *P* = 0.96 for cortical input, *P* = 0.26 for thalamic input) at 25-30 min after beginning of UBP302 application. (**d**) Fractional contribution of the GluR5-KAR-mediated component was unchanged after the induction of ITDP. ITDP in the cortico-amygdala pathway was induced with the TSt-CSt paired stimulation (15 ms interstimulus interval, 90 s at 1 Hz). Twenty minutes after the induction of ITDP, the antagonist of GluR5 subunit-containing KARs UBP 302 (10 μM) was applied for 30 min. Traces are averaged EPSCs recorded before the induction of ITDP (1), after the induction (2) and at the end of UBP 302 application (3). The proportion of the antagonist-sensitive EPSC at the end of UBP 302 application (point 3), that was determined relative to the EPSC amplitude at point 2, was not significantly different from the proportion of the UBP 302-sensitive EPSC without the prior induction of ITDP (n = 4; unpaired *t* test, *P* = 0.22). Error bars indicate s.e.m.

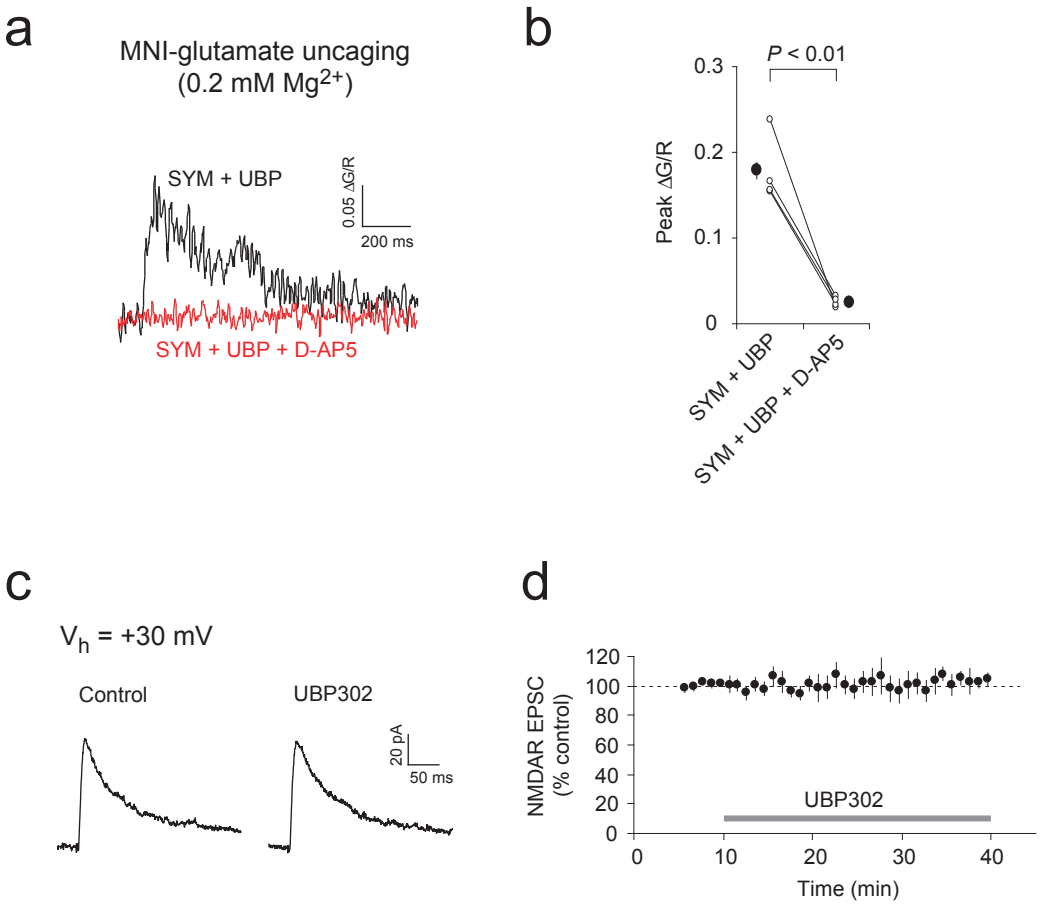

Supplementary Figure 11. Ca^{2+} transients in dendritic spines, recorded in the presence of SYM 2206 and UBP 302, are mediated by activation of NMDARs. (**a**) Using two-photon glutamate uncaging, Ca^{2+} transients were evoked in dendritic spines of LAn neurons in the presence of SYM 2206 (100 μM) and UBP 302 (10 μM). Extracellular Mg^{2+} concentration was 0.2 mM in these experiments. Residual Ca^{2+} transient (ΔG/R) in a single dendritic spine (black trace) was blocked by 50 μM D-AP5 (red trace). (**b**) Summary of imaging experiments as in (**a**), showing values of ΔG/R before (left) and after (right) addition of D-AP5 (n = 4, paired *t* test, $P < 0.01$). (**c**) UBP 302 (10 μM) had no effect on isolated NMDAR EPSCs in the cortical input, which were recorded in the presence of 10 μM NBQX and 50 μM picrotoxin at +30 mV in voltage-clamp mode. Traces are averaged EPSCs recorded before and 30 min after the beginning of UBP 302 application. (**d**) Summary graph of the experiments where the effect of UBP 302 on NMDAR EPSCs was tested (n = 7, paired *t* test, $P = 0.48$ for the baseline EPSC amplitude versus the EPSC amplitude at the end of UBP 302 application). Error bars indicate s.e.m.

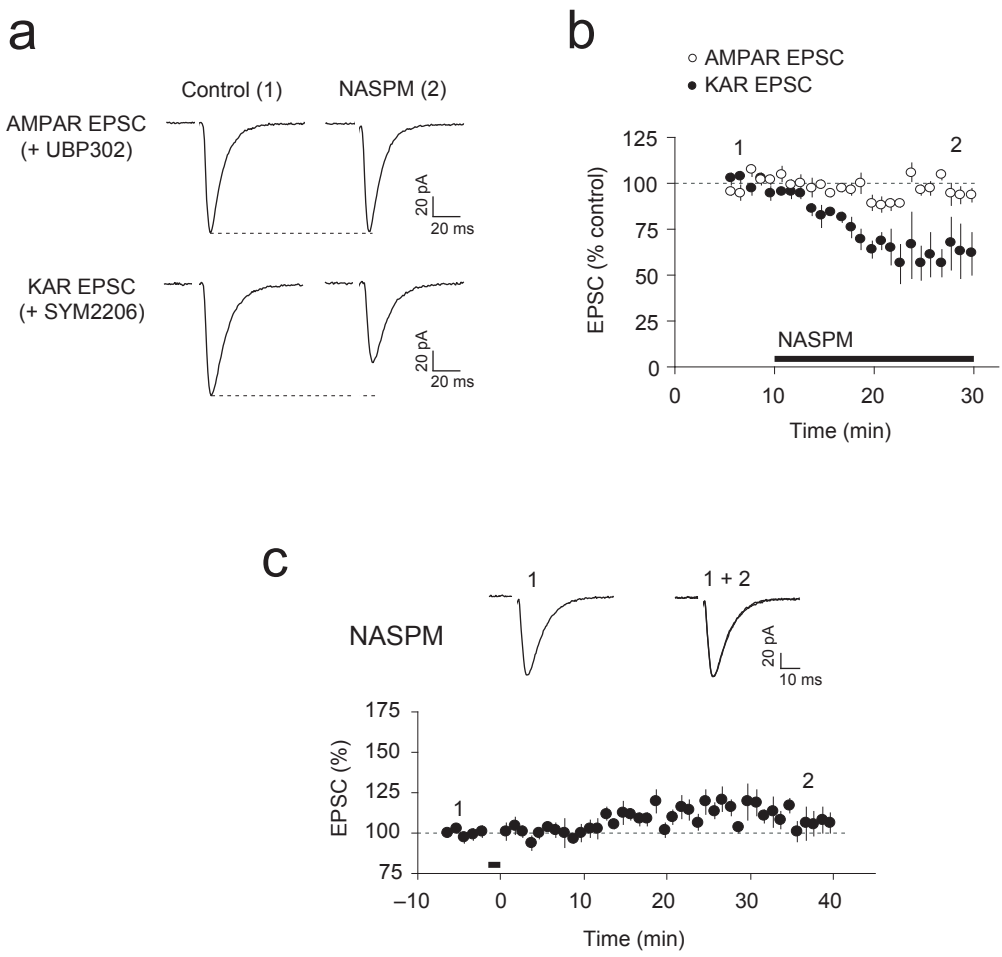

Supplementary Figure 12. Blockade of calcium-permeable KARs suppresses the induction of ITDP. (**a**) The effect of bath-applied 1-naphthyl acetyl spermine (NASPM, 100 μM) on the isolated AMPAR-EPSC (recorded in the presence of 10 μM UBP 302) and KAR-EPSC (recorded in the presence of 100 μM SYM 2206). (**b**) Time course of the effects of NASPM on isolated AMPAR- and KAR-EPSCs. Amplitude of the KAR-EPSC was significantly reduced by NASPM (n = 5, paired *t* test, $P < 0.01$ versus baseline), while the AMPAR EPSC was unaffected (n = 5, paired *t* test, $P = 0.07$ versus baseline). (**c**) Induction of ITDP in the cortical input was blocked in the presence of NASPM (100 μM) included in external solution throughout the experiment (n = 6; paired *t* test, $P = 0.46$ versus baseline). Error bars indicate s.e.m.

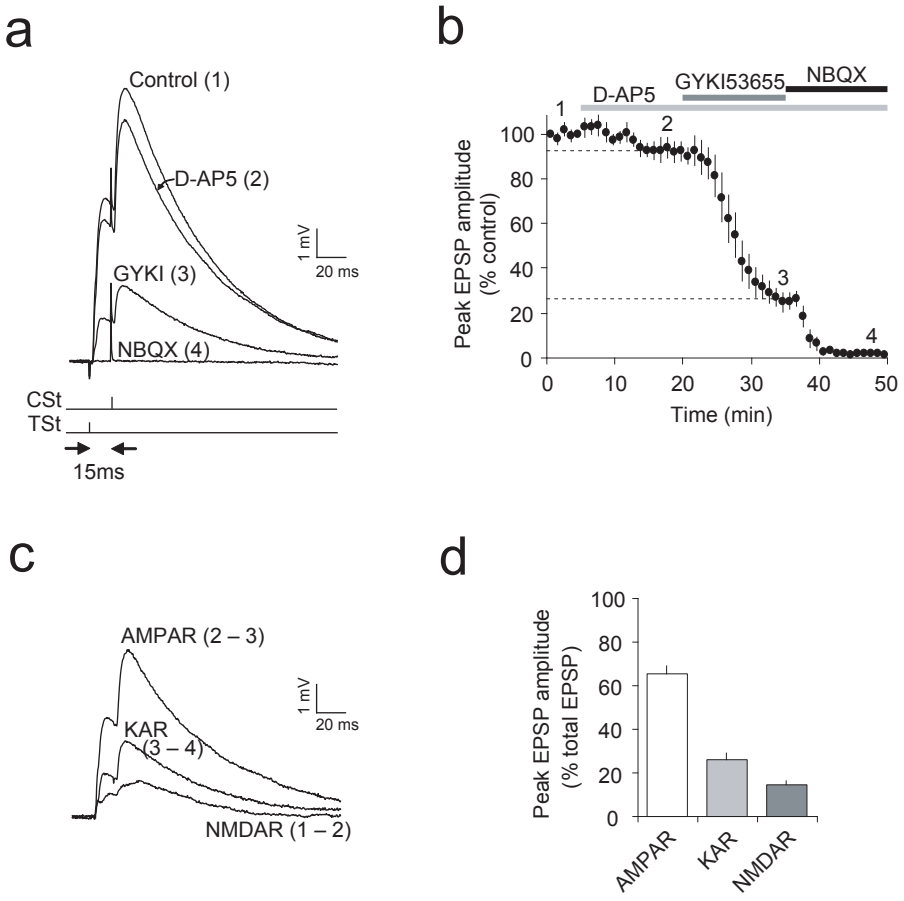

Supplementary Figure 13. Fractional contribution of the AMPAR-, KAR-, and NMDAR-mediated synaptic components to the EPSP during the TSt-CSt paired stimulation. (**a**) Experimental design here was similar to the recordings shown in Fig. 7, but the order of the antagonists' application was changed. Examples of the EPSPs recorded in the LAn neuron in current-clamp mode evoked by paired stimulation of thalamic and cortical inputs with a 15 ms interval under control conditions (1) and in the presence of D-AP5 (50 μM) (2), the AMPAR antagonist GYKI 56355 (10 μM) + D-AP5 (3), and NBQX (10 μM)+ D-AP5 (4). (**b**) Time course of the EPSP depression during application of the antagonists (indicated by bars above the graph). Peak amplitude of EPSPs was normalized to the baseline EPSP amplitude (n = 5). (**c**) Examples of isolated (subtracted) AMPAR-, KAR-, and NMDAR-mediated EPSPs from an experiment shown in (**a**): $EPSP_{AMPAR} = EPSP_{D\text{-}AP5} - EPSP_{GYKI}$; $EPSP_{KAR} = EPSP_{GYKI} - EPSP_{NBQX}$; $EPSP_{NMDAR} = EPSP_{Control} - EPSP_{D\text{-}AP5}$. (**d**) Fractional contribution of the AMPAR-, KAR-, and NMDAR-EPSPs in the compound EPSP (based on the peak amplitude measurements) during paired TSt-CSt stimulation (n = 5). Error bars indicate s.e.m. The peak amplitude of the subtracted NMDAR-mediated component of the compound EPSP was 14 ± 2 % of the control EPSP amplitude (not significantly different from the estimate obtained in the experiments shown in Fig. 7: 12 ± 1 %, n = 6; unpaired *t* test, *P* = 0.85 between two estimates).

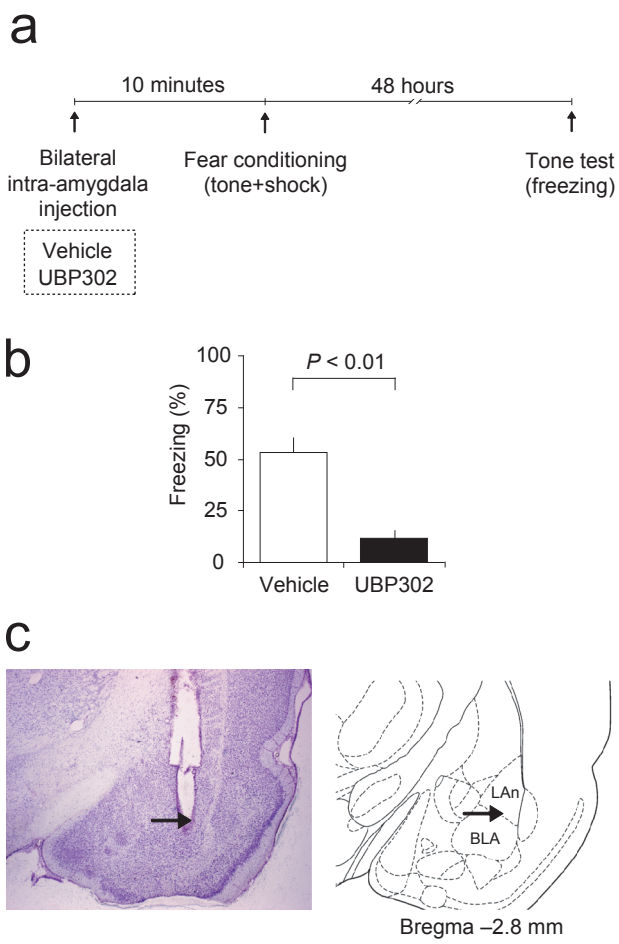

Supplementary Figure 14. Fear conditioning is sensitive to the blockade of GluR5 subunit-containing KARs. (**a**) A diagram depicting the experimental design. (**b**) Freezing responses 48 hr after auditory fear conditioning in rats which received bilateral intra-amygdala microinfusions of the selective GluR5 subunit-containing KAR antagonist, UBP302 (3 μg/side), or vehicle 10 min before conditioning (see Online Methods). Freezing is significantly reduced in the UBP302-treated group compared to the vehicle-injected group (6 rats per group; Mann-Whitney *U* test, $P < 0.01$). (**c**) Placement of the intra-amygdala cannula as determined by Nissl stain in coronal brain sections through the amygdala. Error bars are s.e.m.

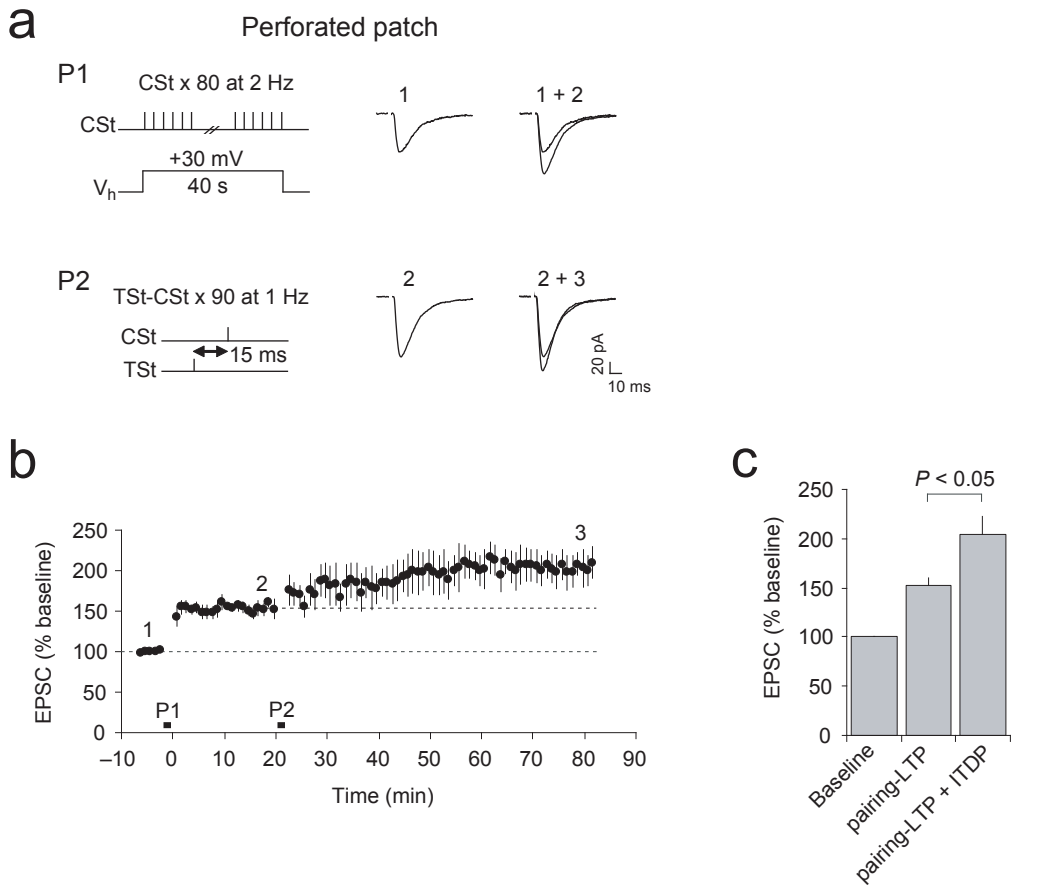

Supplementary Figure 15. Pairing-induced LTP does not occlude the induction of ITDP. (**a** and **b**) The nystatin-based perforated patch-clamp technique was used in these experiments. Pairing of 80 presynaptic pulses, delivered to cortical fibers at a 2-Hz frequency, and postsynaptic depolarization to +30 mV (P1) resulted in potentiation of the cortico-LAn EPSC (recorded at –70 mV) to 153 ± 7 % of the baseline amplitude (n = 5, paired *t* test, $P < 0.01$ versus baseline; traces 1 and 2 in (**a**)). Twenty minutes after the induction of the "pairing LTP", a standard ITDP protocol, consisting of paired stimulation of thalamic and cortical inputs (TSt-CSt) with the 15-ms interval for 90 s at 1 Hz was delivered (P2). This led to further potentiation of the EPSC amplitude (133 ± 7 % of the new baseline immediately before the delivery of ITDP protocol, n = 5, paired *t* test, $P < 0.05$; trace 3 in (**a**)). The magnitude of ITDP under these conditions did not differ from the magnitude of ITDP observed without a prior induction of "pairing-LTP" (unpaired *t* test, $P = 0.72$). These findings indicate that paring-induced LTP does not occlude the induction of ITDP. (**c**) Summary graph showing that amplitude of the cortico-LAn EPSC after the sequential induction of both "pairing-LTP" and ITDP was significantly larger than the amplitude of the EPSC after the induction of "pairing-LTP" alone (n = 5, paired *t* test, $P < 0.05$). Thus, ITDP and conventional (NMDAR-dependent) forms of LTP in the conditioned stimulus pathways may be additive, cooperatively increasing synaptic responses to the auditory CS after fear conditioning. Error bars are s.e.m.